LANGMUIR

pubs.acs.org/Langmuir Article

Fabrication and Characterization of Tumor Nano-Lysate as a Preventative Vaccine for Breast Cancer

Jenna A. Dombroski, Nidhi Jyotsana, Davis W. Crews, Zhenjiang Zhang, and Michael R. King*

Cite This: *Langmuir* 2020, 36, 6531−6539 Read Online

ACCESS | Metrics & More | Article Recommendations

ABSTRACT: Breast cancer is the most common cancer among women in the United States, with late stages associated with the lowest survival rates. The latest stage, defined as metastasis, accounts for 90% of all cancer-related deaths. There is a strong need to develop antimetastatic therapies. TRAIL, or TNF-related apoptosis inducing ligand, has been used as an antimetastatic therapy in the past, and conjugating TRAIL to nanoscale liposomes has been shown to enhance its targeting efficacy. When circulating tumor cells (CTCs) released during metastasis are exposed to TRAIL-conjugated liposomes and physiologically relevant fluid shear stress, this results in rapid cancer cell destruction into cell fragments. We sought to artificially recreate this phenomenon using probe sonication to mechanically disrupt cancer cells and characterized the resulting cell fragments, termed "tumor nano-lysate", with respect to size, charge, morphology, and composition. Furthermore, an in vivo pilot study was performed to investigate the efficacy of tumor nano-lysate as a preventative vaccine for breast cancer in an immunocompetent mouse model.

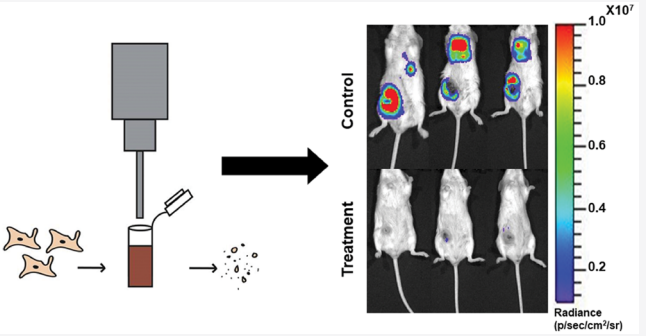

INTRODUCTION

One in eight women in the United States will be diagnosed with breast cancer in her lifetime,[1,2] and breast cancer can also afflict men, although it is less common. Later stages of breast cancer, accompanied by the lowest 5-year survival rates, are defined as distant or metastatic. Metastasis accounts for 90% of all cancer-related deaths.[3] While there has been improvement in the 5-year survival rate for breast cancer, there is still a significant disparity; in fact, while survival rates are 99% for patients diagnosed with local disease, they drop to 27% for metastatic breast cancer.[4] In the process of metastasis, a cancer cell derived from a primary tumor intravasates into the bloodstream as a circulating tumor cell (CTC). CTCs travel through the circulation with the potential to form a secondary tumor in a distant microenvironment.[5] Primarily, metastatic therapies focus on quality of life and prolonged survival for patients, given the severity of the stage of the disease.[2,6,7] However, some novel treatments for metastatic patients have emerged. Current therapies include virotherapy and chimeric antigen receptor (CAR) T and stem cell therapies.[8,9] Additionally, there is a wide array of therapies that hold potential for antimetastatic therapy, such as the delivery of engineered exosomes.[10]

TRAIL therapy can also be used to target CTCs in the bloodstream to prevent the development of cancer metastasis.[11−13] TRAIL functions by binding to death receptors 4 and 5 on cancer cells to induce apoptosis while sparing healthy, noncancerous cells.[14] Conjugating TRAIL to nanoscale liposomes increases its targeting efficiency for CTCs both in vitro and in vivo.[11−13] Cone and plate flow devices were used to apply a physiologically relevant shear stress to cancer cells in vitro to simulate the fluid shear stress of the circulation that CTCs traveling through the bloodstream experience. Through modeling blood flow, cone and plate flow devices are also able to apply a sustained shear rate that increases the sensitivity of cancer cells to TRAIL.[15,16] In images obtained following these experiments, it was shown that CTCs exposed to fluid shear stress (FSS) and TRAIL-conjugated liposomes were disrupted into cancer cell fragments.[16] Normal cells will not produce a similar product, since TRAIL produces apoptosis in cancer cells while sparing most normal cells, and FSS alone will not cause the same effects in such healthy cells.[17] As cancer cell fragments are released into the blood in vivo in response to liposomal TRAIL therapy, it is expected that these bodies are exposing the tumor-associated antigens to cells in the immune system to potentially elicit an immune response.

Received: April 2, 2020
Revised: May 18, 2020
Published: May 21, 2020

https://dx.doi.org/10.1021/acs.langmuir.0c00947
Langmuir 2020, 36, 6531−6539

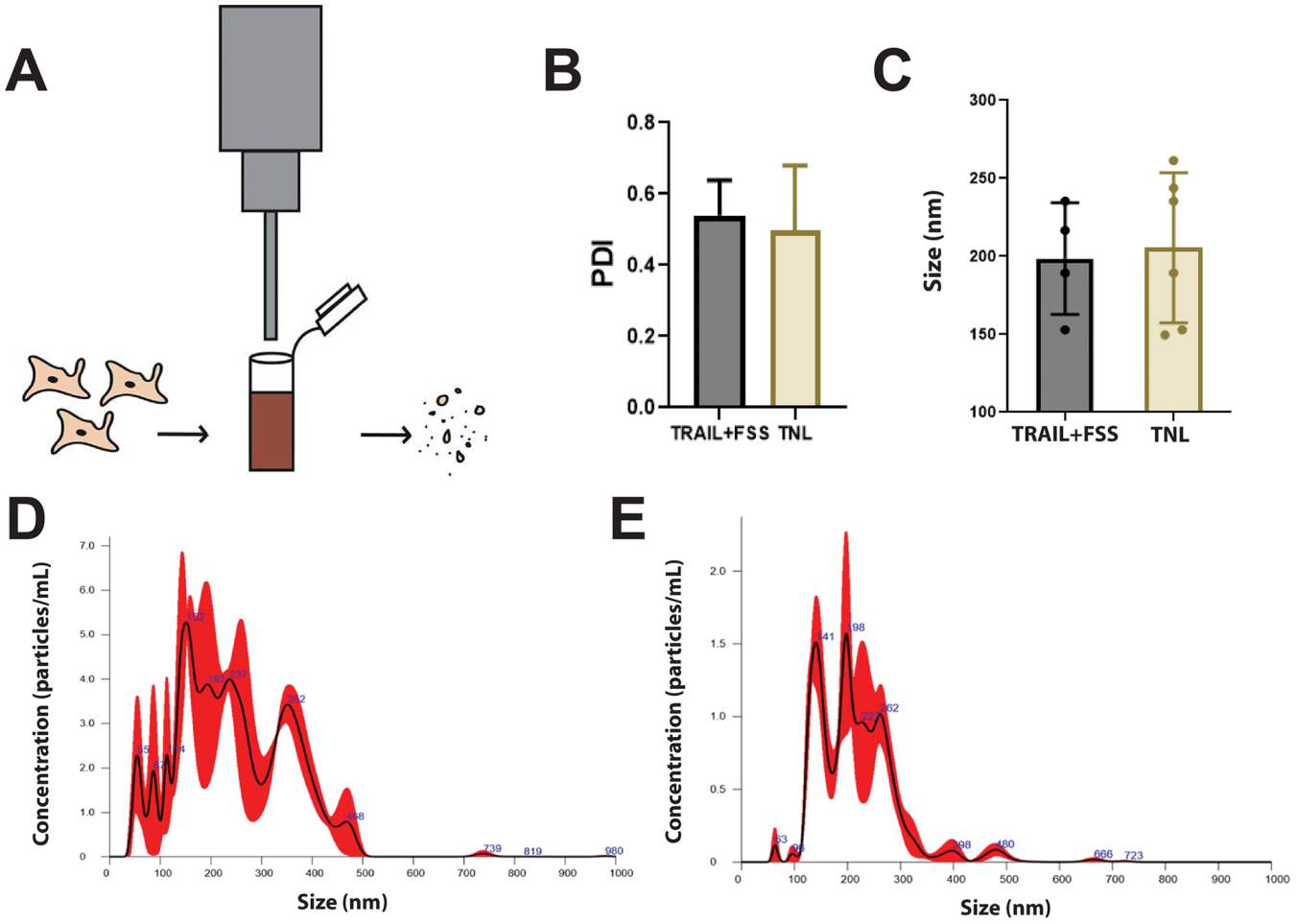

Figure 1. Preparation, polydispersity, and size characterization of TNL. (A) Sonication process for producing cancer cell fragments or tumor nanolysate. (B) Polydispersity index (PDI) of 4T1 cells exposed to TRAIL+FSS and sonication (TNL) had a standard error of 0.04 and 0.06, respectively. The average PDI for the TRAIL+FSS group and TNL group was 0.54 ± 0.10 and 0.50 ± 0.18, respectively. (C) Average particle size as measured by NanoSight, comparing TRAIL+FSS. (D) Representative figure of average TNL size as measured by NanoSight. (E) Representative figure of average size of cancer cell fragments following exposure to TRAIL+FSS. Statistical significance was calculated by using the unpaired *t* test.

Breast cancer treatments can be modeled and tested in vitro and in vivo with a variety of murine models that include cell-line-derived xenografts (CDX), patient-derived xenografts (PDX), syngeneic models, genetically engineered mouse models (GEMM), and humanized models.[18] 4T1 breast cancer is a syngeneic mouse model of mammary carcinoma that is highly invasive and metastatic and can be transplanted orthotopically into the mammary fat pad of a BALB/c mouse for in vivo studies.[19,20] A strength of the 4T1 model is that it allows for the use of an immunocompetent mouse, which is extremely beneficial for studies involving host response and vaccines.[21−23] The metastatic predisposition of the 4T1 model has made it a significant model for circulating tumor cells and antimetastatic therapies, and we have used it for our FSS and TRAIL therapies.[12]

We have shown that TRAIL and FSS can kill 4T1 CTCs in vitro and in vivo with a variety of murine and humanized models.[11−13] Surgical removal of the primary tumor is a common practice in breast cancer treatment. However, postsurgical metastasis poses an immense setback in cancer therapy. Considering that 90% of cancer-related deaths are due to metastasis, antimetastatic therapeutic strategies that can target disseminating tumor cells in the circulation before they can form secondary tumors hold preclinical and clinical potential for cancer patients. Our recent work uses a liposomal formulation functionalized with the adhesion receptor E-selectin and the apoptosis-inducing ligand TNF (tumor necrosis factor)-related apoptosis-inducing ligand (TRAIL) to reduce metastasis following tumor resection in an aggressive triple-negative breast cancer (TNBC) mouse model.[11−13] We demonstrated that minimal administration of E-selectin−TRAIL liposomes can target metastasis in a TNBC model, with primary tumor resection to mimic clinical settings. Our study indicated that TRAIL liposomes, alone or in combination with existing clinically approved therapies, may neutralize distant metastasis of a broad range of tumor types.[11−13] We have found that TRAIL and FSS can kill 4T1 CTCs in vitro.[12] With three doses of TRAIL-conjugated liposomes and removal of the primary tumor, we were able to target CTCs and prevent metastases in vivo in the 4T1 model.[12] Because mice showed no signs of metastases following treatment, we believe that the cell fragments produced during the therapy may aid in immune memory and prevention of tumor development from any remaining CTCs. A downside of using these therapies to evoke immune memory is the potential for issues of resistance and harmful side effects, so finding a way to generate similar cell products without TRAIL treatment would be beneficial.[24]

https://dx.doi.org/10.1021/acs.langmuir.0c00947
Langmuir 2020, 36, 6531−6539

A

	Mean Zeta Potential (mV)	Standard Deviation (mV)
TRAIL +FSS	-3.7	1.5
TNL	-4.1	1.3

B

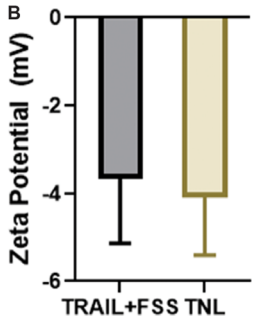

Figure 2. Zeta potential measurements for cells exposed to TRAIL+FSS and sonication. (A) Table of values for mean zeta potential (mV) and standard deviation for zeta potential (mV) for 4T1 cells exposed to TRAIL and FSS and 4T1 cells exposed to sonication (TNL). The standard error was 0.6 mV for the TRAIL+FSS group and 0.5 mV for the TNL group. (B) Quantification of zeta potential (mV) for 4T1 cells exposed to TRAIL and FSS and 4T1 cells exposed to sonication (TNL).

With the goal to recreate this phenomenon artificially, we used probe sonication to mechanically disrupt cancer cells. We characterized these nanoscale cancer cell fragments, which we have termed "tumor nano-lysate" (TNL). The TNL were characterized by size, charge, morphology, and composition. We also performed an in vivo pilot study to investigate the efficacy of the tumor nano-lysate as a preventative vaccine for 4T1 breast cancer in a mouse model.

RESULTS

Preparation and Characterization of TNL. The fluid shear stress (FSS) of blood flow can be modeled by using a cone and plate flow device.[25] Using this system, we have recapitulated the stresses that circulating tumor cells (CTCs) experience in the bloodstream in vivo and used this to test the efficacy of antimetastatic treatments for a variety of cancer types.[11,13] Combining 4T1 cancer cells with TRAIL therapy and applying FSS via cone and plate flow device result in cancer cell fragments in vitro. With the ultimate goal to recreate the phenomenon of cancer cell fragmentation that results from the combination of FSS and exposure to TRAIL, we sought to lyse cancer cells artificially. Cells can be lysed by a variety of means, including chemical and mechanical methods of lysis.[26,27] Lysing cells artificially would offer many advantages over the use of cell fragments derived from exposing 4T1 cells to TRAIL and FSS. These advantages include avoiding potential issues such as cell resistance to TRAIL and negative side effects such as hepatotoxicity.[24]

With the goal to mimic the exposure to forces applied by shear stress and a desire to prevent further changes to the cells beyond lysis, we chose mechanical lysis via ultrasonic frequencies. In previous literature, when lysing cells via sonication, 40−50% amplitude was recommended, as were short pulses of sonication followed by time for cooling.[28,29] The sonication process was optimized by using different sonicating and cooling times as recommended by the literature.[28,30−33] After sonication, samples were measured by polydispersity index (PDI) and size. Sonicating times that provided fragments larger than the desired size range of 175−275 nm or with a PDI larger than 0.75 were not selected. Because short pulses and cooling cycles were suggested, we selected a series of 2 and 10 s pulses, finding that they had similar size range and PDI. Three pulses of 10 s sonication and 10 s cooling, as suggested by the literature, resulted in the least amount of visible foaming and provided ample cooling time, as it was not hot to the touch.[29,33,34] TNL was kept on ice during sonication and cooling to keep the samples cooled. For the mechanical disruption of our cancer cells, 4T1 breast cancer cells suspended in PBS were mechanically disrupted via probe sonication for a combined total of 30 s of sonication at 50% amplitude, with time for cooling, and kept on ice (Figure 1A). At these settings, we were able to minimize both sample foaming and heating.

Cancer Cells Disrupted by Sonication Become Nanometer Sized and Highly Dispersed. The resulting sonicated cancer cells were characterized by size via Zetasizer and NanoSight and then compared to cells fragmented after exposure to TRAIL and FSS. Zetasizer measurements revealed a high polydispersity (PDI) in sample size for both conditions, which was expected due to randomness of the lysis during the sonication process (Figure 1B). For 4T1 cells exposed to FSS and TRAIL, the average polydispersity index was 0.54, while the average polydispersity index for sonicated cells, or tumor nano-lysate (TNL), was 0.50. PDI is defined as the weight-average divided by the number-average molecular weight and characterizes the breadth of molecular weight distribution.[35] A high PDI lies close to 1.0 and indicates a highly dispersed size range of measured samples. Therefore, these results indicate that the samples were not monodispersed and that a Zetasizer is not the optimal measurement tool for determining the average particle size. As a result, the NanoSight, with an ability to provide more accurate size range and concentrations of nanoparticles, was used to characterize the particle size distribution of each sample.

With the Zetasizer, TRAIL+FSS lysate was measured to be 200−230 nm in diameter, while TNL were measured to be 185−275 nm. With the aid of the NanoSight, the sonicated cancer cell product was measured to have a standard error of 19.7 nm and have an average diameter of 205 ± 48.2 nm. Similarly, cancer cell product exposed to FSS and TRAIL had a standard error of 17.9 nm and was measured to have an average diameter of 199 ± 35.6 nm (Figure 1C−E). From this information, we were able to conclude that we could closely recapitulate the size range of fragmented cancer cells resulting from the in vitro FSS modeled system.

Measured Surface Charge of Sonicated Cancer Cells Is Slightly Negative. The zeta potential was measured and compared for the sonicated cancer cells and cancer cells exposed to TRAIL and FSS. Using electrophoretic light scattering via Zetasizer, we determined the surface charge for each sample. It was observed that the zeta potential was slightly negative for both samples, although the standard deviation of each sample was relatively high (Figure 2A,B). The mean zeta potential for 4T1 cells exposed to TRAIL and fluid shear stress

https://dx.doi.org/10.1021/acs.langmuir.0c00947
Langmuir 2020, 36, 6531−6539

(FSS) was −3.7 ± 1.5 mV and −4.1 ± 1.3 for 4T1 cells exposed to sonication (TNL). The negative charge of cell fragments is unsurprising given that the surface charge of cells is also negative, and mechanical lysis should not alter that property.[27,36] While the standard deviation for 4T1 cells exposed to either TRAIL+FSS or sonication was high, interestingly, there was not a significant difference between the standard deviations of the zeta potential values.

Imaging of Sonicated Cancer Cells Reveal Membrane-Bound Vesicles. The cell fragments derived from the sonication of cancer cells, referred to as tumor nano-lysate (TNL), were imaged by using transmission electron microscopy (TEM). Using microscopy, we were able to visualize what appeared to be membrane-encapsulated vesicles among the tumor nano-lysate (Figure 3). TEM shows two of

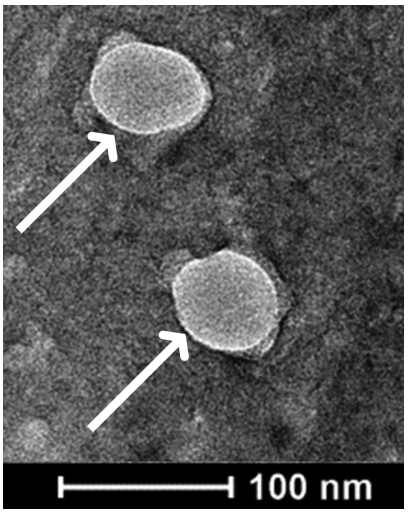

Figure 3. Transmission electron microscopy image of 4T1 breast cancer cells after sonication. White arrows indicate the presence of membrane-bound vesicles in the sample of sonicated cells.

the smaller-sized TNL particles, at around 100 nm in size. The creation of these membranous features has been observed in the past when sonicating cells via probe sonication, with an ability to form liposome-like structures as a result of the disruption of the cell membrane and then spontaneous re-formation of a bilayer due to electrostatic interactions.[37]

Sonicated Cancer Cells Contain Protein Contents Similar to 4T1 Cells Lysed by RIPA Buffer. The sonicated cancer cells were then characterized for composition and contents. Mass spectrometry was used to examine the protein contents, comparing the sonicated cancer cells to a sample of control 4T1 cells lysed with RIPA lysis buffer. Fragments derived from TRAIL+FSS treated cells were not used as a comparison group since there was insufficient protein for accurate measurements via mass spectrometry. Among the most common proteins in the sample of sonicated cancer cells were albumin, cytoplasmic actin, α-enolase, elongation factor 1-α1, galectin, mitochondrial HSP 60 kDa, and vimentin (Figure 4A). The greatest percent deviations of protein concentrations of the TNL from the RIPA buffer control were calculated from the 1317 analyzed proteins of each sample. The extremely low differences in concentration demonstrate that the proteins from tumor nano-lysate are not significantly different than the proteins found in the RIPA control. (Figure 4B). One of the most common proteins, Myosin-9, is expected as it is commonly upregulated in cancer cells as it is a protein responsible for growth and embryonic development and plays a role in aiding in cancer cell motility.[38,39] The group of heat shock proteins (HSP mitochondrial, HSPA8, and HSP90B) is also expected, as these are often diagnostic markers of cancer and implicated in a variety of cancer-promoting phenomena.[40]

Sonicated Cancer Cells Do Not Affect the Viability of Healthy Epithelial or Primary Tumor Tissue in Vitro. Apoptosis assays were performed to test the toxicity of the sonicated cancer cells and determine whether the formulation would induce an unwanted effect of cell death. An Annexin V apoptosis assay compared the effects of cells treated with tumor nano-lysate (TNL) to cells treated with a vehicle control (PBS). First, healthy mouse mammary epithelial tissue (EpH4-Ev) cells were exposed to TNL suspended in PBS. At 1 mg TNL/10 mg live EpH4-Ev cells, EpH4-Ev cells exposed to TNL showed an average cell viability of 75 ± 5.3% compared to 79 ± 3.3% for the PBS-treated control, with standard errors 2.38% and 1.47%, respectively. At 2 mg TNL/5 mg live EpH 4-Ev cells, cell viability was 75 ± 4.0% for TNL-treated cells and 79 ± 2.0% for PBS-treated cells. Standard errors were 1.79% and 0.89%, respectively. Both the higher and lower concentrations of TNL revealed no significant increase in apoptosis or loss of cell viability when compared to PBS (Figure 5A). These TNL dosages are much higher than the dose used in the in vivo study, thus representing a conservative toxicity test.

In addition to healthy cells, we also investigated the apoptotic effects of TNL on breast cancer cells in vitro. When 4T1 breast cancer cells were exposed to TNL suspended in PBS, the resulting Annexin V apoptosis assay showed no significant toxic effects on these primary tumor cells compared to the PBS-treated control (Figure 5B). At 1 mg TNL/10 mg live 4T1 cells, TNL-treated 4T1 cells showed an average viability of 85 ± 1.8%, compared to 86 ± 2.0% for the PBS control, with standard errors calculated to be 0.74% and 0.89%, respectively. The higher 2 mg TNL/5 mg live 4T1 cells dose produced similar results, with an average cell viability of 84 ± 3.6% for TNL-treated cells and 83 ± 6.2% for PBS-treated cells. Standard errors were 1.45% and 2.55%, respectively. These results support the idea that this tumor nano-lysate may well act as a preventative method by exposing the immune system to tumor-associated antigens, rather than as a mechanism of directly targeting the primary tumor itself.

One Dose of TNL Vaccine Prior to Tumor Inoculation Reduces Tumor Growth, Delays Metastasis, and Increases Survival for Mice Challenged with Breast Cancer Xenograft. Having developed TNL that physically mimic the naturally created apoptotic bodies resulting from TRAIL treatment in the presence of FSS, we proceeded to test their biological activity in vivo. We hypothesized that the tumor-associated antigens from the 4T1 cells would induce an adaptive immune response. Prior to the animal trial, an immunological assay for T cell activation was performed to ensure that the TNL would not put undue strain on the immune system of the mice. This study tested for the upregulation of CD25 and CD69 in lymphocytes, T cell markers for late and early activation, respectively. Spleenocytes harvested from BALB/c mice were exposed for 24 h to three different conditions: (1) PBS vehicle control, (2) 4T1 cells exposed to fluid shear stress and TRAIL (FSS+TRAIL) suspended in PBS, and (3) tumor nano-lysate suspended in

https://dx.doi.org/10.1021/acs.langmuir.0c00947
Langmuir 2020, 36, 6531−6539

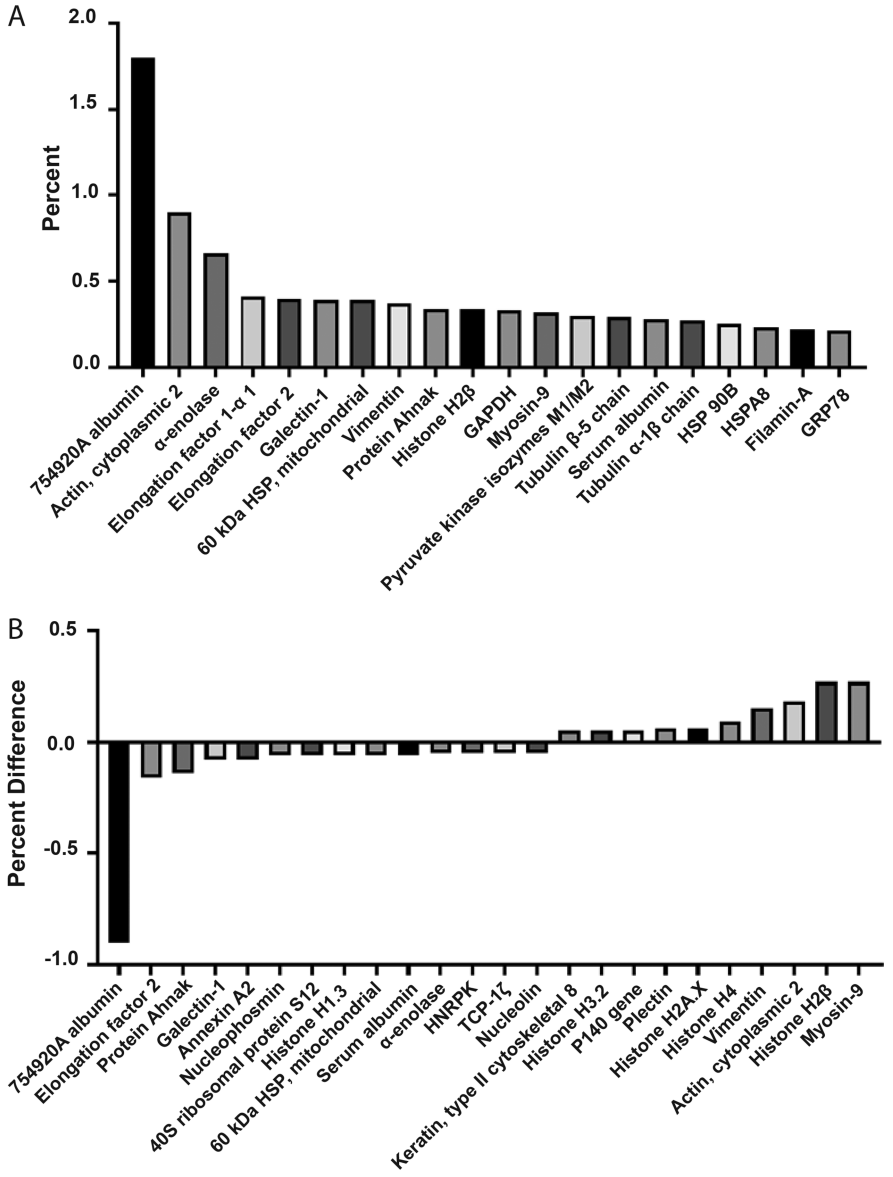

Figure 4. Content characterization of tumor nano-lysate via mass spectrometry. (A) The 25 highest protein concentrations for sonicated cancer cell sample. Albumin is present in large amounts because of the RPMI cell culture media. (B) Greatest percent differences between TNL and control of 4T1 cells lysed by RIPA buffer. The low differences in concentration indicate that the tumor nano-lysate is not significantly different than the proteins found in the control.

PBS (TNL). No significant difference was found between the three conditions, indicating that these treatments were sufficiently safe for the pilot study (Figure 6A).

Ten days before tumor inoculation with 4T1-Luc breast cancer cells, mice in the tumor nano-lysate group received one dose of TNL suspended in PBS, while the remaining mice were untreated. Following tumor inoculation, mice were monitored via bioluminescence imaging (BLI), and the tumor size was measured via calipers once palpable (Figure 6B). BLI data showed more rapid tumor growth for control mice that did not receive the injection of TNL (Figure 6C). Results of the pilot study revealed significantly reduced tumor volume for mice that received a dose of tumor nano-lysate compared to control (Figure 6D). Metastasis from the primary tumor was also observed much earlier for untreated mice, delayed an average of 10 days for mice that received one dose of the vaccine (Figure 6E). The median overall survival was extended an average of 7 days for the vaccinated group, and they did not require humane sacrifice as early as their untreated counterparts (Figure 6F). Although survival was delayed, eventually the mice in both groups required humane sacrifice. There were no visible changes to the appearance, behavior, or health of the mice that would be evidence of adverse side effects. Thus, a single pretreatment with TNL can delay the onset of primary tumor development, delay metastasis, and prolong survival in mice.

■ DISCUSSION

We were able to successfully create nanoscale lysate derived from tumor cells using sonication. This TNL was found to have a negative zeta potential, with its size and charge similar to cancer cell particles created through the application of TRAIL and fluid shear stress via cone and plate flow device. Although the standard deviation of the zeta potential was high compared to the charge, this is to be expected. While the lipid

https://dx.doi.org/10.1021/acs.langmuir.0c00947
Langmuir 2020, 36, 6531−6539

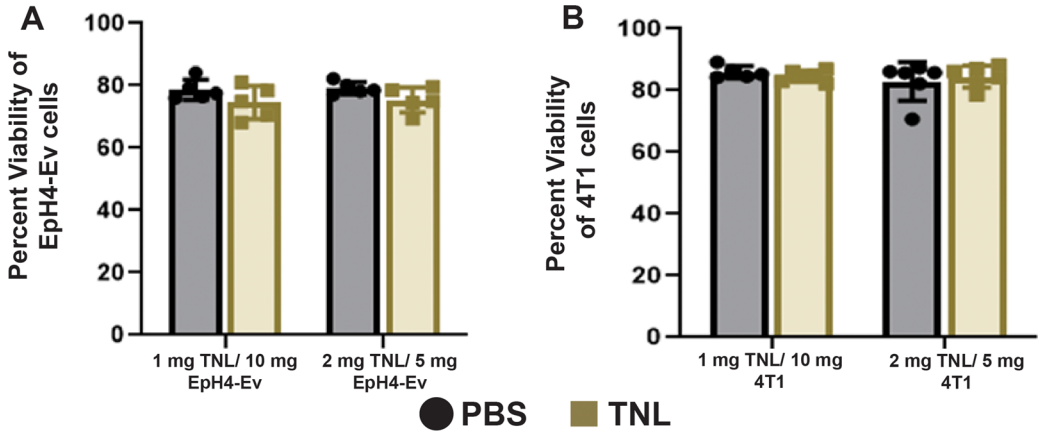

Figure 5. Apoptosis assay of healthy epithelial and tumor breast tissue. (A) No significant difference in cell viability was observed between EpH4-Ev epithelial tissue exposed to either dosage of TNL when compared to EpH4-Ev cells exposed to PBS buffer. (B) Similarly, there was no significant difference in cell viability for 4T1 breast cancer cells exposed to either concentration of TNL when compared to 4T1 cells exposed to PBS buffer. These experiments were performed in duplicate. The significance was determined by using a two-way ANOVA in GraphPad Prism. ***$p < 0.005$.

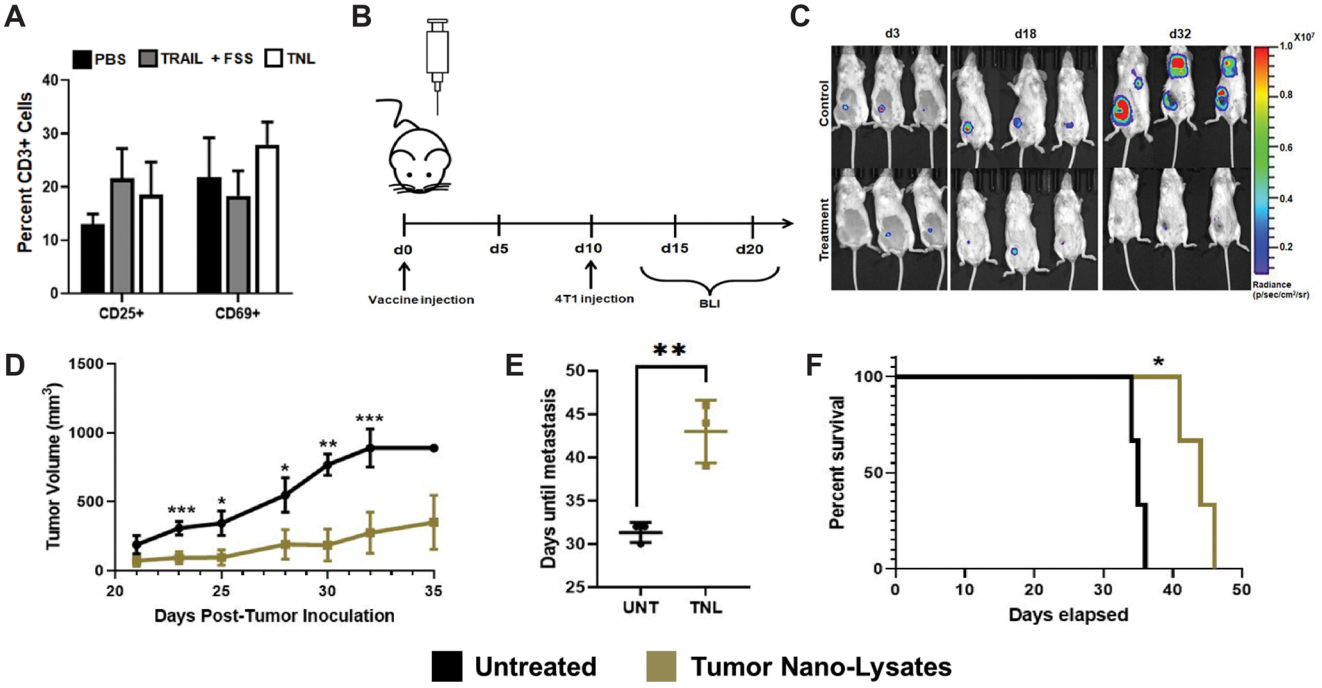

Figure 6. In vivo pilot study for vaccinated mice inoculated with 4T1 tumor. (A) In vitro assay comparing T cell activation for PBS vs TNL-treated spleenocytes. (B) Timeline for in vivo study (C) IVIS imaging of mice using bioluminescent and Luc-expressing 4T1 cells. (D) Tumor size over time for measurements taken via caliper. (E) Days of metastasis observation post-tumor inoculation. (F) Survival curve. Statistical significance determined by two-tailed ANOVA. *$p < 0.05$, **$p < 0.01$, and ***$p < 0.005$.

bilayer defining the TNL particle structures should resemble the negatively charged surface of the parent cell plasma membrane, the relatively high variance in zeta potential that was observed may reflect the variety of cytoplasmic contents that have associated with the TNL surface during the chaotic sonication process. As desired, we were able to closely recapitulate these characteristics of cell fragments resulting from exposing 4T1 cells to TRAIL and FSS. To further validate this study, performing a rechallenge experiment on mice given our TRAIL therapy would provide further insight to compare the two conditions. Nevertheless, our method does not require the use of TRAIL, limiting potential issues such as resistance and side effects that could result from the therapeutic.

Following sonication, the lysate was observed to form membrane-bound vesicles. The proteins present in the TNL sample, consistent with those found in 4T1 cells lysed with RIPA buffer, could prove effective for evoking a protective response once exposed to memory cells in the immune system. These characteristics likely make TNL favorable to uptake by antigen presenting cells (APCs) or other immune cells, which may aid in adaptive immunity in vivo.

While little research has been dedicated to the characterization of cell lysate in the past, artificially developed apoptotic bodies are the closest resemblance to TNL and fragments derived from TRAIL+FSS.[41,42] They have shown similar wide size ranges and morphologies as the cell fragments in this

https://dx.doi.org/10.1021/acs.langmuir.0c00947
Langmuir 2020, 36, 6531−6539

study, although microvesicles show nearly identical average size and morphology to our TNL.[42]

No evidence of toxicity was found when healthy breast tissue was exposed to lower or higher (1:10−2:5 mg TNL/mg EpH 4-Ev) concentrations of tumor nano-lysate when compared to PBS control. Similarly, when 4T1 breast cancer cells were exposed to two different concentrations of TNL derived from 4T1 cells subjected to sonication (1:10−2:5 mg TNL/mg 4T1), no toxic effects or decrease in cell viability was found. This evidence suggested that TNL could proceed with in a preliminary in vivo study and that any observed effect would likely occur through immune cell response rather than a direct effect on the primary tumor cells. While the success of our in vitro toxicity assays prompted an in vivo study, we plan on performing future mouse studies to analyze the in vivo effects of TNL. These studies should investigate localized and systemic reactions that could take place upon exposure to TNL. However, we do not expect that cell lysate would be toxic, since they are recreating the apoptosis resulting from TRAIL+FSS treatments; 50−70 billion cells undergo apoptosis each day in the adult human, which does not result in toxicity in patients.[43] Cell lysate and apoptotic bodies from a variety of cell types including T cells, stem cells, skin cells, brain cells, and peripheral blood mononuclear cells (PBMCs) have been injected in vivo in several recent studies, and none of the studies raised toxicity concerns.[34,43−45]

Although mice treated with a single dose of the TNL vaccine ultimately developed primary tumors and metastases, this study represents an important step forward and indicates that these mechanically produced cell fragments hold potential as a preventative vaccine for triple negative breast cancer.

It would be interesting to further explore the mechanisms behind the effectiveness of these tumor-derived lysate. These should consist of studies on immune cell activation in response to TNL exposure. Preliminary studies suggest that a B cell response drives the response (data not shown), and further investigations into this mechanism should be conducted. In addition, an analysis of immune cell infiltration to the tumor site may reveal discrepancies in the tumor microenvironments between mice in the control and vaccinated groups. A future study to test if sonicated normal cells would produce a similar preventative effect could act as a control to more conclusively elucidate whether TNL are successful due to the specific presentation of tumor-specific antigens.[46]

MATERIALS AND METHODS

Production of Sonicated Cancer Cells. 4T1 breast cancer cells (ATCC, CRL-2539) were cultured in RPMI 1640 growth media (Thermo Fisher Scientific) with 10% fetal bovine serum and 1% penicillin−streptomycin. The cells were plated, grown to 80% confluency, and lifted from the plate surface. Cells were centrifuged at 1200 rpm for 5 min, with the cell pellet resuspended in phosphate buffered saline (PBS). Cells in the pellet were counted and diluted with PBS to achieve a final concentration of 1 million cells in 1 mL of PBS. Using a Fisherbrand Sonic Dismembrator Model 50, we sonicated cells at 1/2 max sonication 3 times for 10 s each, for a total of 30 s of sonication time. Temperature rise of the sample in the test tube was attenuated by using a beaker full of ice. Immediately after sonication, cells were placed on ice. The sonicated cancer cells, termed tumor nano-lysate (TNL), were stored at −20 °C.

Size, Dispersity, and Charge Measurements. The Vanderbilt Institute of Nanoscale Science and Engineering (VINSE) Analytical Laboratory was used for size and dispersity measurements. Nanoparticle tracking analysis (NTA) for particle size and concentration was performed using a Malvern Panalytical NanoSight NS300. Samples were further diluted with PBS to 1:100. A DLS Malvern Nano ZS (Zetasizer Nano ZS) was used to measure sample size, dispersity, and electrostatic charge. Size and dispersity measurements were obtained using Malvern Disposable microcuvettes. A disposable folded capillary cell was used to take zeta potential measurements.

Morphology. An Osiris transmission electron microscope (TEM) from the Vanderbilt Institute for Nanoscale Science and Engineering Advanced Imaging facility was used to analyze the morphology of the tumor nano-lysate material. Samples were prepared by using negative staining, placing the sample on a copper grid, and adding phosphotungstic acid (PTA) solution.[47] This process surrounds the sample with electron dense materials, revealing the surface contrast between darker stain and lighter specimen.

Contents Characterization. A complete mass spectrometry analysis was performed for all of the identified proteins in the control sample and the tumor nano-lysate sample. Mass spectrometry analysis was performed at the Vanderbilt Mass Spectrometry Research Center (MSRC) Core at the Vanderbilt University School of Medicine. Scaffold Proteome Software identified 1317 proteins. The top 20 proteins were analyzed and compared for this study. Albumin was identified as the highest concentration of protein, although that is due to the presence of cell culture medium. The full file containing all of the proteins identified will be provided on request.

Annexin V Assay. EpH4-Ev (ATCC CRL-3063) and 4T1 (ATCC CRL-2539) cells were used to test the toxicity of tumor nano-lysate on normal epithelial and triple negative breast cancer cells, respectively. Annexin V assay was performed to test the apoptotic effects of TNL on each cell type. 50000 cells were plated and exposed to 1 mg TNL/10 mg live cells or 2 mg TNL/5 mg live cells, equivalent to 5 and 20 μL of TNL solution (1 million 4T1 cells/1 mL PBS), respectively. Cells in the control groups were exposed to 5 or 20 μL of PBS buffer. Cells were lifted and centrifuged at 1200 rpm for 5 min, and the pellet was resuspended in 150 μL of PBS with calcium and magnesium. 5 μL of annexin and 5 μL of propidium iodide (PI) were added to the samples, with unstained, annexin V, and PI controls. After 15 min of incubation in the dark at room temperature, 100 μL of PBS was added to each of the samples and then run through a Guava EasyCyte flow cytometer (Millipore, Billerica, MA). Flow cytometry data analyses were performed using FlowJo software.

Immune Assay. Spleenocytes were isolated from the spleen of healthy BALB/c mice following an established protocol.[48] Cells were plated in 24-well plates at 50000 cells per well. Three wells were dedicated to controls (unstained, FITC isotype, and APC isotype). Each sample was tested in triplicate. 5 μL of PBS was added to six wells for vehicle controls for the two different markers (CD25 and CD69). Similarly, 1:10 mg TNL/mg spleenocytes, equivalent to 5 μL of TNL (1 million sonicated 4T1 cells in 1 mL of PBS), were incubated in six wells. Finally, 1:10 mg TRAIL+FSS lysate/mg spleenocytes were incubated in six wells of the plate. After 24 h, the cells were lifted and centrifuged at 1200 rpm for 5 min and resuspended in 100 μL of PBS. All cells were then stained for 1 h without light exposure with 2 μL of CD3 and 2 μL of CD25 or CD69. Samples were processed through a Guava EasyCyte flow cytometer, and data were analyzed by using FlowJo software.

In Vivo Pilot Study. Eight week old female BALB/c mice were purchased from the Jackson Laboratory (Bar Harbor, ME) and were cared for by veterinary staff at the Department of Animal Care (DAC) at Vanderbilt University. Mice in the control group (n = 3) and experimental group (n = 3) experienced identical housing conditions and care regimens. This pilot study was approved by Institutional Review Board, protocol #M1700009-00. Mice were euthanized at humane end points. These end points were determined based on tumor size and recommendation by veterinary staff at the DAC.

4T1 Orthotopic Tumor Model and TNL Treatment. Mice were injected with one dose of TNL (10^5 sonicated 4T1 cells in 100 μL of PBS) via the tail vein 10 days prior to tumor inoculation. For tumor inoculation, 30000 4T1 breast cancer cells transfected with luciferase were suspended in 50 μL of PBS and injected into the anatomical right fourth mammary fat pad of each mouse. During the

https://dx.doi.org/10.1021/acs.langmuir.0c00947
Langmuir 2020, 36, 6531−6539

inoculation, mice were anesthetized for 5−10 min via continuous inhalation of isoflurane. Luciferase expression in the mice was monitored via bioluminescence imaging on an in vivo imaging system (IVIS Lumina III, PerkinElmer Inc.) twice per week, following a subcutaneous injection of 100 μL of D-luciferin (150 mg/kg). Calipers were used to measure the length (l) and width (w) of the tumor, with tumor volume estimated as $(l \times w^2)/2$. Metastases were considered as bioluminescent signals in locations other than the mammary fat pad. These indicate cancer spread to distant organs. Days when mice were observed to begin showing signs of metastases were recorded and compared.

Data Analysis. Data are presented as mean ± standard deviation, and statistical significance is determined in GraphPad Prism by two-tailed ANOVA, unless otherwise indicated. *$p < 0.05$, **$p < 0.01$, and ***$p < 0.005$.

AUTHOR INFORMATION

Corresponding Author

Michael R. King − *Department of Biomedical Engineering, Vanderbilt University, Nashville, Tennessee 37235, United States;* orcid.org/0000-0002-0223-7808; Email: mike.king@vanderbilt.edu

Authors

Jenna A. Dombroski − *Department of Biomedical Engineering, Vanderbilt University, Nashville, Tennessee 37235, United States*

Nidhi Jyotsana − *Department of Biomedical Engineering, Vanderbilt University, Nashville, Tennessee 37235, United States*

Davis W. Crews − *Department of Biomedical Engineering, Vanderbilt University, Nashville, Tennessee 37235, United States*

Zhenjiang Zhang − *Department of Biomedical Engineering, Vanderbilt University, Nashville, Tennessee 37235, United States*

Complete contact information is available at: https://pubs.acs.org/10.1021/acs.langmuir.0c00947

Notes

The authors declare no competing financial interest.

ACKNOWLEDGMENTS

We thank Majed A. Massad for help with 4T1 cell culture. This work was supported by NIH Grant R01 CA203991 awarded to M.R.K.

REFERENCES

(1) DeSantis, C. E.; Ma, J.; Goding Sauer, A.; Newman, L. A.; Jemal, A. Breast cancer statistics, 2017, racial disparity in mortality by state. *Ca-Cancer J. Clin.* **2017**, *67* (6), 439−448.

(2) Harbeck, N.; Gnant, M. Breast cancer. *Lancet* **2017**, *389* (10074), 1134−1150.

(3) Chaffer, C. L.; Weinberg, R. A. A perspective on cancer cell metastasis. *Science (Washington, DC, U. S.)* **2011**, *331* (6024), 1559−1564.

(4) Schairer, C.; Mink, P. J.; Carroll, L.; Devesa, S. S. Probabilities of death from breast cancer and other causes among female breast cancer patients. *J. Natl. Cancer Inst.* **2004**, *96* (17), 1311−1321.

(5) Fidler, I. J. The pathogenesis of cancer metastasis: the 'seed and soil' hypothesis revisited. *Nat. Rev. Cancer* **2003**, *3*, 453−458.

(6) Accordino, M. K.; et al. Use and costs of disease monitoring in women with metastatic breast cancer. *J. Clin. Oncol.* **2016**, *34* (24), 2820−2826.

(7) Sledge, G. W. Curing Metastatic Breast Cancer. *J. Oncol. Pract.* **2016**, *12* (1), 6−10.

(8) Turcotte, S.; Rosenberg, S. A. Immunotherapy of Metastatic Solid Cancers. *Adv. Surg.* **2011**, *45*, 341−360.

(9) Park, G. T.; Choi, K. C. Advanced new strategies for metastatic cancer treatment by therapeutic stem cells and oncolytic virotherapy. *Oncotarget* **2016**, *7* (36), 58684−58695.

(10) Zhang, Z.; Dombroski, J. A.; King, M. R. Engineering exosomes to target cancer metastasis. *Cell. Mol. Bioeng.* **2020**, *13*, 1.

(11) Mitchell, M. J.; Wayne, E.; Rana, K.; Schaffer, C. B.; King, M. R. TRAIL-coated leukocytes that kill cancer cells in the circulation. *Proc. Natl. Acad. Sci. U. S. A.* **2014**, *111* (3), 930−935.

(12) Jyotsana, N.; Zhang, Z.; Himmel, L. E.; Yu, F.; King, M. R. Minimal dosing of leukocyte targeting TRAIL decreases triple-negative breast cancer metastasis following tumor resection. *Sci. Adv.* **2019**, *5* (7), eaaw4197.

(13) Wayne, E. C.; et al. TRAIL-coated leukocytes that prevent the bloodborne metastasis of prostate cancer. *J. Controlled Release* **2016**, *223*, 215−223.

(14) Almasan, A.; Ashkenazi, A. Apo2L/TRAIL: Apoptosis signaling, biology, and potential for cancer therapy. *Cytokine Growth Factor Rev.* **2003**, *14* (3−4), 337−348.

(15) Hope, J. M.; Lopez-Cavestany, M.; Wang, W.; Reinhart-King, C. A.; King, M. R. Activation of Piezo1 sensitizes cells to TRAIL-mediated apoptosis through mitochondrial outer membrane permeability. *Cell Death Dis.* **2019**, *10* (11), 837.

(16) Mitchell, M. J.; King, M. R. Fluid shear stress sensitizes cancer cells to receptor-mediated apoptosis via trimeric death receptors. *New J. Phys.* **2013**, *15*, 015008.

(17) Ashkenazi, A.; et al. Safety and antitumor activity of recombinant soluble Apo2 ligand. *J. Clin. Invest.* **1999**, *104* (2), 155−162.

(18) Holen, I.; Speirs, V.; Morrissey, B.; Blyth, K. In vivo models in breast cancer research: Progress, challenges and future directions. *Dis. Models & Mech.* **2017**, *10* (4), 359−371.

(19) Pulaski, B. A.; Ostrand-Rosenberg, S. Mouse 4T1 Breast Tumor Model. *Curr. Protoc. Immunol.* **2000**, *39*, 20.2.1−20.2.16.

(20) Park, M. K.; Lee, C. H.; Lee, H. Mouse models of breast cancer in preclinical research. *Lab. Anim. Res.* **2018**, *34* (4), 160.

(21) Finn, O. J. Immuno-oncology: Understanding the function and dysfunction of the immune system in cancer. *Ann. Oncol.* **2012**, *23*, viii6.

(22) Clem, A. S. Fundamentals of vaccine immunology. *J. Glob. Infect. Dis.* **2011**, *3* (1), 73−78.

(23) Semenkow, S.; et al. An immunocompetent mouse model of human glioblastoma. *Oncotarget* **2017**, *8* (37), 61072−61082.

(24) von Karstedt, S.; Montinaro, A.; Walczak, H. Exploring the TRAILs less travelled: TRAIL in cancer biology and therapy. *Nat. Rev. Cancer* **2017**, *17* (6), 352.

(25) Mitchell, M. J.; King, M. R. Computational and experimental models of cancer cell response to fluid shear stress. *Front. Oncol.* **2013**, DOI: 10.3389/fonc.2013.00044.

(26) Brown, R. B.; Audet, J. Current techniques for single-cell lysis. *J. R. Soc., Interface* **2008**, DOI: 10.1098/rsif.2008.0009.focus.

(27) Islam, M. S.; Aryasomayajula, A.; Selvaganapathy, P. R. A Review on Macroscale and Microscale Cell Lysis Methods. *Micromachines* **2017**, *8* (3), 83.

(28) Browne, J. A.; Harris, A.; Leir, S. H. An optimized protocol for isolating primary epithelial cell chromatin for ChIP. *PLoS One* **2014**, *9* (6), e100099.

(29) Kwon, Y. C.; Jewett, M. C. High-throughput preparation methods of crude extract for robust cell-free protein synthesis. *Sci. Rep.* **2015**, DOI: 10.1038/srep08663.

(30) Pchelintsev, N. A.; Adams, P. D.; Nelson, D. M. Critical Parameters for Efficient Sonication and Improved Chromatin Immunoprecipitation of High Molecular Weight Proteins. *PLoS One* **2016**, *11* (1), e0148023.

(31) "Protein Purification", European Molecular Biology Laboratory. [Online]. Available: https://www.embl.de/pepcore/pepcore_services/protein_purification/extraction_clarification/cell_lysate_ecoli/.

(32) Introduction to Thermo Scientific Cell Lysis Solutions. In *Thermo Scientific Pierce Cell Lysis Technical Handbook*; 2009; p 6.
(33) "Cell and Tissue Lysate Preparation", Proteintech. [Online]. Available: https://www.ptglab.com/media/2724/protocols-for-web_lysate-preparation_v3.pdf.
(34) El-Amouri, S. S.; Cao, P.; Miao, C.; Pan, D. Secreted Luciferase for In Vivo Evaluation of Systemic Protein Delivery in Mice. *Mol. Biotechnol.* **2013**, *53* (1), 63−73.
(35) Rane, S. S.; Choi, P. Polydispersity Index: How Accurately Does It Measure the Breadth of the Molecular Weight Distribution? *Chem. Mater.* **2005**, *17*, 926.
(36) Pekker, M.; Shneider, M. N. The surface charge of a cell lipid membrane. *J. Phys. Chem. Biophys.* **2015**, *5*, 177.
(37) Dua, J. S.; Rana, P. A. C.; Bhandari, D. A. K. Liposome: methods of preparation and applications. *Int. J. Pharm. Stud. Res.* **2012**, *III* (II), 14−20.
(38) Pecci, A.; Ma, X.; Savoia, A.; Adelstein, R. S. MYH9: Structure, functions and role of non-muscle myosin IIA in human disease. *Gene* **2018**, *664*, 152−167.
(39) Li, Y. R.; Yang, W. X. Myosins as fundamental components during tumorigenesis: Diverse and indispensable. *Oncotarget* **2016**, *7* (29), 46785−46812.
(40) Ciocca, D. R.; Calderwood, S. K. Heat shock proteins in cancer: diagnostic, prognostic, predictive, and treatment implications. *Cell Stress Chaperones* **2005**, *10* (2), 86−103.
(41) SUCHORSKA, W. M.; LACH, M. S. The role of exosomes in tumor progression and metastasis. *Oncol. Rep.* **2016**, *35*, 1237.
(42) Osteikoetxea, X. Improved Characterization of EV Preparations Based on Protein to Lipid Ratio and Lipid Properties. *PLoS One* **2015**, *10*, e0121184.
(43) Liu, D.; et al. Circulating apoptotic bodies maintain mesenchymal stem cell homeostasis and ameliorate osteopenia via transferring multiple cellular factors. *Cell Res.* **2018**, *28* (9), 918−933.
(44) Youniss, F. M.; et al. Near-Infrared Imaging of Adoptive Immune Cell Therapy in Breast Cancer Model Using Cell Membrane Labeling. *PLoS One* **2014**, *9* (10), e109162.
(45) de Carvalho Bittencourt, M.; Perruche, S.; Contassot, E.; Fresnay, S.; Baron, M.-H.; Angonin, R.; Aubin, F.; Herve, P.; Tiberghien, P.; Saas, P.; et al. Intravenous injection of apoptotic leukocytes enhances bone marrow engraftment across major histocompatibility barriers. *Blood* **2001**, *98* (1), 224−230.
(46) Vigneron, N. Human Tumor Antigens and Cancer Immunotherapy. *BioMed Res. Int.* **2015**, *2015*, 948501.
(47) Paliwal, S. R.; et al. Estrogen-Anchored pH-Sensitive Liposomes as Nanomodule Designed for Site-Specific Delivery of Doxorubicin in Breast Cancer Therapy. *Mol. Pharmaceutics* **2012**, *9* (1), 176−186.
(48) Lim, J. F.; Berger, H.; Su, I. Isolation and Activation of Murine Lymphocytes. *J. Visualized Exp.* **2016**, DOI: 10.3791/54596.

https://dx.doi.org/10.1021/acs.langmuir.0c00947
Langmuir 2020, 36, 6531−6539